COMPDYN 2011
III ECCOMAS Thematic Conference on
Computational Methods in Structural Dynamics and Earthquake Engineering
M. Papadrakakis, M. Fragiadakis, V. Plevris (eds.)
Corfu, Greece, 25–28 May 2011

IMPACT MODELING BY MANIFOLD APPROACH IN EXPLICIT TRANSIENT DYNAMICS

Timo J. Saksala[1*], Jari M. Mäkinen[2],

[1,2] Department of Mechanics and Design,
Tampere University of Technology
P.O. Box 589, FI-33101 Tampere, Finland
[1]timo.saksala@tut.fi,
[2]jari.m.makinen@tut.fi

Keywords: Explicit dynamics, Contact mechanics, Lagrange multiplier method, Penalty method, Constraint manifold.

Abstract. *In this paper we study numerically different methods to impose contact constraints in explicit dynamics. The traditional methods, the penalty method and the more recent forward increment Lagrange multiplier method, are compared, in their performance and accuracy, to a direct elimination method based on the theory of manifolds. The idea of the method is that when a contact constraint is active the solution lies on the boundary of the contact manifold generated by contact constraints. Then the contact problem can be solved with the elimination of additional degrees of freedom. This elimination technique can be viewed as a parameterization of the contact manifold. We show numerically that in the case of a rigid impactor, the elimination method is highly more efficient than the forward Lagrange multiplier method since the latter leads to a coupled system of equations for solving the Lagrange multipliers while both methods produce similar results. In the present work the elimination method is also developed for the impact problem of deformable bodies and the performance of the different methods are compared in numerical simulations of the longitudinal impact of thick bars. The modified Euler method is employed in solving the equations of motion in time.*

1 INTRODUCTION

The traditional method to impose contact constraints in explicit transient dynamics is the penalty function method. It is, however, an approximate method and has an adverse effect on the numerical stability of explicit integration. For this reason, Carpenter et al. [1] introduced a modification of Lagrange multiplier method, called Forward Increment Lagrange Multiplier method (FILM), which is compatible with explicit time integrators and does not affect the stability of integration. The idea of the method is to refer the kinematic contact constraints one time step ahead of the equations of motion and the Lagrange multipliers. With general contact interfaces, this method leads to a coupled system of equations for the Lagrange multipliers. Therefore, if the number of contact pairs is large it is not effective.

In this paper we present an alternative and efficient method for impact modeling in explicit transient dynamics. The method, called here DME (Direct Manifold Elimination method) is based on the theory of manifolds. Contact constraints, i.e. the displacement inequalities, generate a constraint manifold with a boundary [2]. When a contact constraint is active the solution lies on the boundary of the contact manifold. This method was employed by Saksala & Mäkinen [3] in case of a rigid piston impacting an elasto-viscoplastic damaging domain. In that case, the contact constraints, i.e. the impenetrability conditions between the piston node and rock surface nodes, were eliminated. In the present paper, this formulation is also performed in the case of a deformable impactor and the node-to-node contact interface.

The developed technique is implemented in 2D (axisymmetric) case. In the numerical examples involving impacts between linear elastic bodies and dynamic indentation by a rigid indenter, the accuracy and efficiency of the manifold method is compared to the penalty function method and the forward increment Lagrange multiplier method. The modified Euler explicit integrator is used for solving the FE discretized equations of motion in time.

2 IMPOSITION OF CONTACT CONSTRAINTS

In this section we describe the traditional methods, the penalty method and the more recent forward increment Lagrange multiplier method, as well as the manifold method to impose kinematic contact constraints in explicit time integration setting. The background for the manifold method is elaborated only to the level required for understanding how the method arises. Linear elasticity and small displacements are assumed for simplicity.

2.1 Modified Euler method for explicit time integration

The explicit modified Euler time integrator is chosen for solving the equations of motion. The response of the system using this method is computed by [4]:

$$\begin{aligned} \ddot{\mathbf{u}}^{t} &= \mathbf{M}^{-1}\left(\mathbf{f}_{\text{ext}}^{t} - \mathbf{C}\dot{\mathbf{u}}^{t} - \mathbf{f}_{\text{int}}^{t}\right) \\ \dot{\mathbf{u}}^{t+\Delta t} &= \dot{\mathbf{u}}^{t} + \Delta t\ddot{\mathbf{u}}^{t} \\ \mathbf{u}^{t+\Delta t} &= \mathbf{u}^{t} + \Delta t\dot{\mathbf{u}}^{t+\Delta t} \end{aligned} \tag{1}$$

where $\mathbf{M}$ is the lumped mass matrix, $\mathbf{C}$ is the damping matrix (set zero here), $\mathbf{f}_{\text{int}}, \mathbf{f}_{\text{ext}}$ are the internal and external force vectors, respectively, and $\mathbf{u}$ is the displacement vector while a dot above it denotes time derivative.

2.2 Forward increment Lagrange multiplier and penalty method

The classical Lagrange multiplier method is incompatible with explicit time integrators. For this reason, Carpenter et al. [1] introduced a modification, called here forward increment

Lagrange multiplier method, which is compatible with explicit methods. The idea of the method is to refer the kinematic contact constraints one time step ahead of Lagrange multipliers as:

$$\begin{aligned} &\mathbf{M}\ddot{\mathbf{u}}^{t} + \mathbf{C}\dot{\mathbf{u}}^{t} + \mathbf{f}_{\text{int}}^{t} = \mathbf{f}_{\text{ext}}^{t} - \mathbf{G}^{\text{T}}\boldsymbol{\lambda}^{t} \\ &\mathbf{G}\mathbf{u}^{t+\Delta t} - \mathbf{b} = \mathbf{0} \end{aligned} \tag{2}$$

where **b** is the vector containing the initial distances between the contact node pairs (which are known in advance), **G** is the kinematic contact constraint matrix consisting, usually, of the normal vectors of the contact surfaces, and $\boldsymbol{\lambda}$ is the Lagrange multiplier vector having the physical interpretation of contact forces. On substituting (1) into (2) gives, after some algebra:

$$\begin{aligned} \ddot{\mathbf{u}}^{t} &= \tilde{\ddot{\mathbf{u}}}^{t} - \mathbf{M}^{-1}\mathbf{G}^{\text{T}}\boldsymbol{\lambda}^{t} \\ \dot{\mathbf{u}}^{t+\Delta t} &= \dot{\mathbf{u}}^{t} + \Delta t\ddot{\mathbf{u}}^{t} \\ \mathbf{u}^{t+\Delta t} &= \mathbf{u}^{t} + \Delta t\dot{\mathbf{u}}^{t+\Delta t} \end{aligned} \tag{3}$$

where

$$\begin{aligned} \tilde{\ddot{\mathbf{u}}}^{t} &= \mathbf{M}^{-1}\left(\mathbf{f}_{\text{ext}}^{t} - \mathbf{C}\dot{\mathbf{u}}^{t} - \mathbf{f}_{\text{int}}^{t}\right) \\ \tilde{\mathbf{u}}^{t+\Delta t} &= \mathbf{u}^{t} + \Delta t\dot{\mathbf{u}}^{t} + \Delta t^{2}\tilde{\ddot{\mathbf{u}}}^{t} \\ \left(\Delta t^{2}\mathbf{G}\mathbf{M}^{-1}\mathbf{G}^{\text{T}}\right)\boldsymbol{\lambda}^{t} &= \mathbf{G}\tilde{\mathbf{u}}^{t+\Delta t} - \mathbf{b} \rightarrow \boldsymbol{\lambda}^{t} \end{aligned} \tag{4}$$

This method belongs to the class of predictor-corrector methods in that, first, the acceleration and displacement of the system are predicted as if there were no contacts. Then, the contact forces are solved based on the virtual penetration. Finally, the acceleration is corrected by subtracting the contribution of the contact forces and the response of the system is updated.

It should be noted that this method is fully explicit only when the node-to-node contact interface is used. In this case, with the lumped mass matrix, the equations for solving the Lagrange multipliers in (4) are uncoupled, i.e. matrix $\Delta t^{2}\mathbf{G}\mathbf{M}^{-1}\mathbf{G}^{\text{T}}$ is diagonal. With more general contact interfaces a coupled system of equations must be solved. Thus, computational efficiency of this method considerably depends on the type of contact interface. The efficiency can be, however, greatly increased, at the expense of accuracy and stability however, if the Penalty method is employed in the contact force calculation. Accordingly, the third equation in (4) and Lagrange multiplier in (3) is replaced by

$$\mathbf{f}_{\text{cont}}^{t} = p\left(\mathbf{G}\tilde{\mathbf{u}}^{t+\Delta t} - \mathbf{b}\right) \tag{5}$$

where p is the problem dependent penalty coefficient. Other equations go unaltered.

2.3 Direct elimination method based on theory of manifolds

Different kinematic relations of constraint equations are shown in Figure 1, where geometric constraints include all holonomic and the unilateral constraints, which are given by inequality equations with the function of time and a generalized place vector only. Unilateral constraints arise when modeling a kinematic relation between bodies in contact.

Contact constraints, i.e. the displacement inequalities, generate a contact manifold with a boundary. When a contact constraint is active the solution lies on the boundary of the contact manifold. Next, the formal definition of the contact manifold is given.

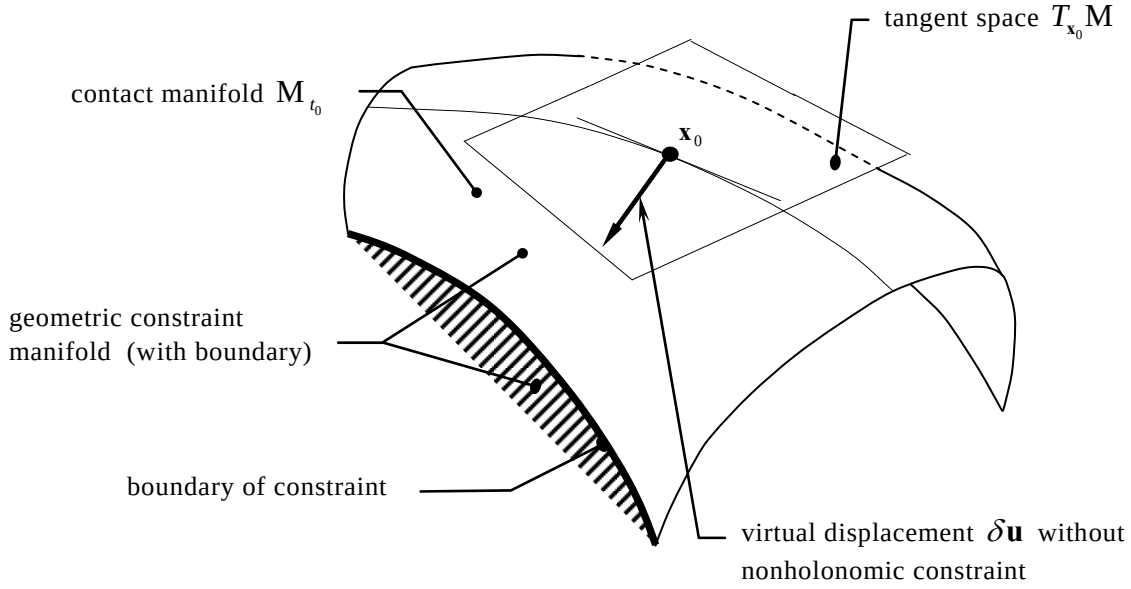

Figure 1: Geometric interpretation of constraints.

Definition for contact manifold: The geometric constraint equations induce a *d*-manifold that is defined by:

$$\mathrm{M} := \left\{ \mathrm{t} \times \mathbf{u} \in \mathbf{R} \times \mathrm{E}^n \mid \mathbf{h}(t, \mathbf{u}) \leq \mathbf{0} \in \mathrm{E}^{n-d} \right\} \tag{6}$$

The contact manifold is a *d*-dimensional smooth manifold with time as 1-parameter family. The contact manifold at fixed time $t = t_0$ is denoted by M_{t_0}.

In our case, the unilateral constraint equations are simply $\mathbf{h}(t, \mathbf{u}) = \mathbf{G}\mathbf{u}^t - \mathbf{b}$. The Lagrange multiplier method and the penalty method, described in the previous section, are conventional methods to impose the contact constraints. However, the contact problem can also be solved with the elimination of additional degrees of freedom. This elimination technique can be viewed as a parameterization of the contact manifold.

In the present paper, we have only node-to-node contacts with straight interfaces (lines) between bodies *A* and *B* and both bodies can be deformable or one of them can be rigid depending on the application. In both cases, the solution procedure begin with the detection of active contacts by checking the violation of the equation

$$\mathbf{G}\tilde{\mathbf{u}}^{t+\Delta t} - \mathbf{b} \geq \mathbf{0} \tag{7}$$

where the predicted displacement is as in Equation (4). Next, two different schemes to compute the nodal displacements, velocities and accelerations are presented. The first one is for the case in which the other body is rigid, thus representing usually a tool used for indentation, and the second is for the impact of deformable bodies.

Case 1 (B is a rigid body, say a punch): If any contact constraint is active, say *i*, then this nodal displacement u_i^A of the body *A* is eliminated by solving the active constraint equation (7) with respect to u_i^A as:

$$
\begin{aligned}
u_i^A &= u_i^B - b_i \\
\dot{u}_i^A &= \dot{u}_i^B \\
\ddot{u}_i^A &= \ddot{u}_i^B = \sum f_{\mathrm{tot},i} / M_i
\end{aligned}
\tag{8}
$$

where $\sum f_{\mathrm{tot},i}$ and $M_i = \sum m_i$ are the total force and mass related to the active contact constraints, i.e. the summation is over the degrees of freedom of the active constraints i.

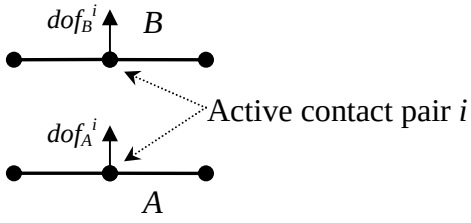

Figure 2: Illustration of node-to-node contact interface.

Case 2 (A and B are deformable bodies): When an active contact pair, say i, is detected according to Equation (7), the acceleration and displacement in the vertical degrees of freedom (dof_B^i and dof_A^i in Figure 2) of the nodes in contact are calculated as:

$$
\begin{aligned}
\hat{u}_i^B &= \hat{u}_i^A = \tfrac{1}{2}\left(u_i^B + u_i^A\right) \\
\ddot{\hat{u}}_i^B &= \ddot{\hat{u}}_i^A = f_{\mathrm{tot},i} / (m_i^A + m_i^B)
\end{aligned}
\tag{9}
$$

where $f_{\mathrm{tot},i} = \mathbf{f}_{\mathrm{tot}}(dof_A^i) + \mathbf{f}_{\mathrm{tot}}(dof_B^i)$ and $m_i^A + m_i^B = \mathbf{M}(dof_A^i) + \mathbf{M}(dof_B^i)$ are the total force and mass related to the active contact pair i with m_i^A and m_i^B being the nodal point masses of the active constraint i for the body A and B, respectively.

As to the velocities, they can be solved from the equations provided by elementary physics of colliding rigid bodies:

$$
\begin{aligned}
m_i^A \dot{u}_i^A + m_i^B \dot{u}_i^B &= m_i^A \hat{\dot{u}}_i^A + m_i^B \hat{\dot{u}}_i^B \\
e(\dot{u}_i^A + \dot{u}_i^B) &= \hat{\dot{u}}_i^A + \hat{\dot{u}}_i^B
\end{aligned}
\tag{10}
$$

where e is the coefficient of restitution with $e = 1$ for elastic collision and $e = 0$ for perfectly inelastic collision. By the elimination technique presented, the degrees of freedom of the problem reduce by one for each active constraint.

Finally, the detection of separation of the active contact constraint can be examined via the nodal internal forces. The separation occurs when the nodal internal force is a tractive force. The tractive force converts the active constraint inactive.

3 NUMERICAL EXAMPLES

In this section the performance of the different methods to impose contact constraints are compared in numerical simulations involving low-velocity impact. First, the performance of the manifold method is demonstrated in the rigid punch indentation problem with varying number of contact constraints. Then, the problem of longitudinal impact of thick cylindrical bars is simulated and the accuracy of the methods is compared with each other and to the analytical solution as well. The material is assumed rigid and/or linear elastic. All the simulations are performed with self-written Matlab (64-bit 2009a version) codes using a Windows Vista pc equipped with 2.60 GHz AMD Phenom™ II X3 710 processor and 8.0 GB of RAM.

3.1 Rigid punch indentation problem

The indentation problem with a rigid punch described in Figure 3 is solved with the FILM, DME and Penalty methods. Axisymmetry of the problem is exploited and CST elements are used in the mesh. The material of the indented domain is linear elastic. The punch is assumed rigid while it is modeled as a single node.

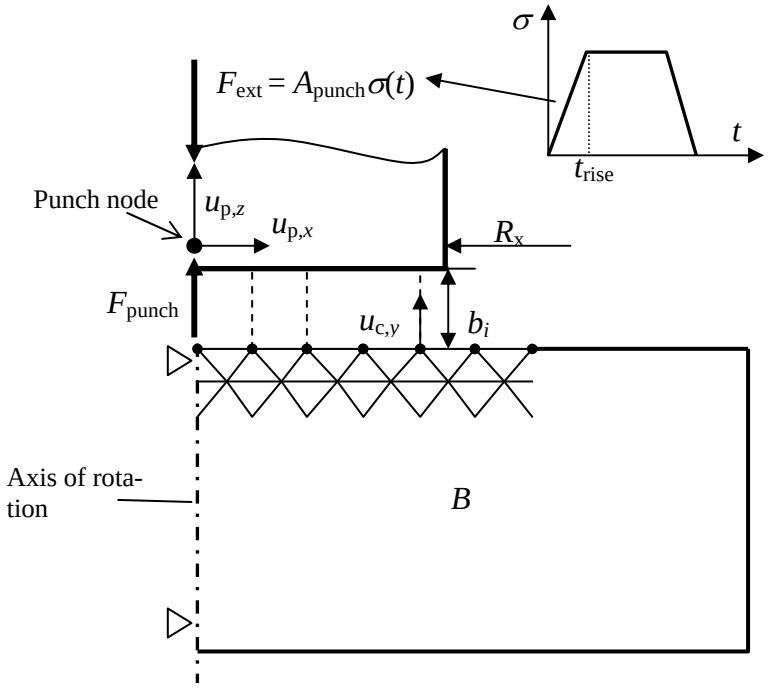

Figure 3: Indentation with a rigid punch.

The external stress pulse, $\sigma(t)$, is used to simulate the impact of the rigid punch to the deformable domain B. As multiplied by the cross sectional area of the indenter A_{punch}, an external force, F_{ext}, to be applied to the punch node is obtained. Moreover, the force that resists the punch penetration into domain B, the contact force F_{punch}, needs to be solved during the solution process. Thus, the equation of motion for the punch node, with its motional degrees of freedom $u_{p,x}$, $u_{p,z}$, to be added to the FE discretized equation of motion, can be written as:

$$m_p \ddot{u}_{p,z} = F_{ext} - F_{punch} \tag{11}$$

where m_p is a computational mass attached to the punch node. The value of this mass must be small enough so that it doesn't affect the solution and big enough to maintain the mass matrix well-conditioned.

The geometry of the punch (indenter) is defined as b_i, i.e. the distances between the punch node and the contact nodes on the indented domain boundary. Thus, using the notation in Figure 3, the kinematic contact constraints can be written in form:

$$u_{\mathrm{c},z} - u_{\mathrm{p},z} = b_i \tag{12}$$

Equations of this form are written for all contact nodes and, consequently, the constraint equation of form **Gu** = **b** is obtained. As there is only one DOF (friction is not taken into account) associated to the punch node, the system of constraint equations is coupled. This system is solved (when using the FILM method) using the Matlab backslash operation. The contact computations are performed as explained in Section 2.

Next, the problem described in Figure 3 is simulated with varying number of contact constraints (achieved easily by different values of radius R_z) using the mesh consisting of 22060 CST elements shown in Figure 4.

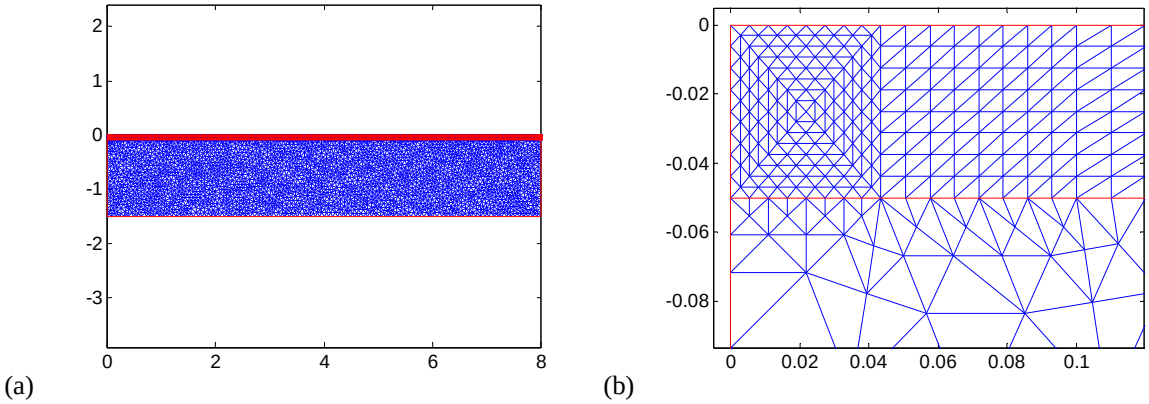

(a) (b)

Figure 4: CST mesh (a) and a detail (b).

The material parameters are: E = 200 GPa, ν = 0.3 and ρ = 7850 kg/m^3. A computational mass of 0.1 kg is used for the punch node mass m_p. A time step $\Delta t = 3.64\times10^{-7}$ s is chosen to keep the computations stable. Three different simulations are carried out in what follows, corresponding to three different number of contact constraints: Sim1 with 107 (R_z = 1 m), Sim2 with 308 (R_z = 3 m) and Sim3 with 610 (R_z = 6 m) contact constraints. The analysis time is $400\Delta t = 1.457\times10^{-4}$s. The stress pulse amplitude is 200 MPa while its duration, rise and descent times are 1×10^{-4}s, 1×10^{-5}s, respectively. The results of the simulations for Sim1 are presented in Figure 5.

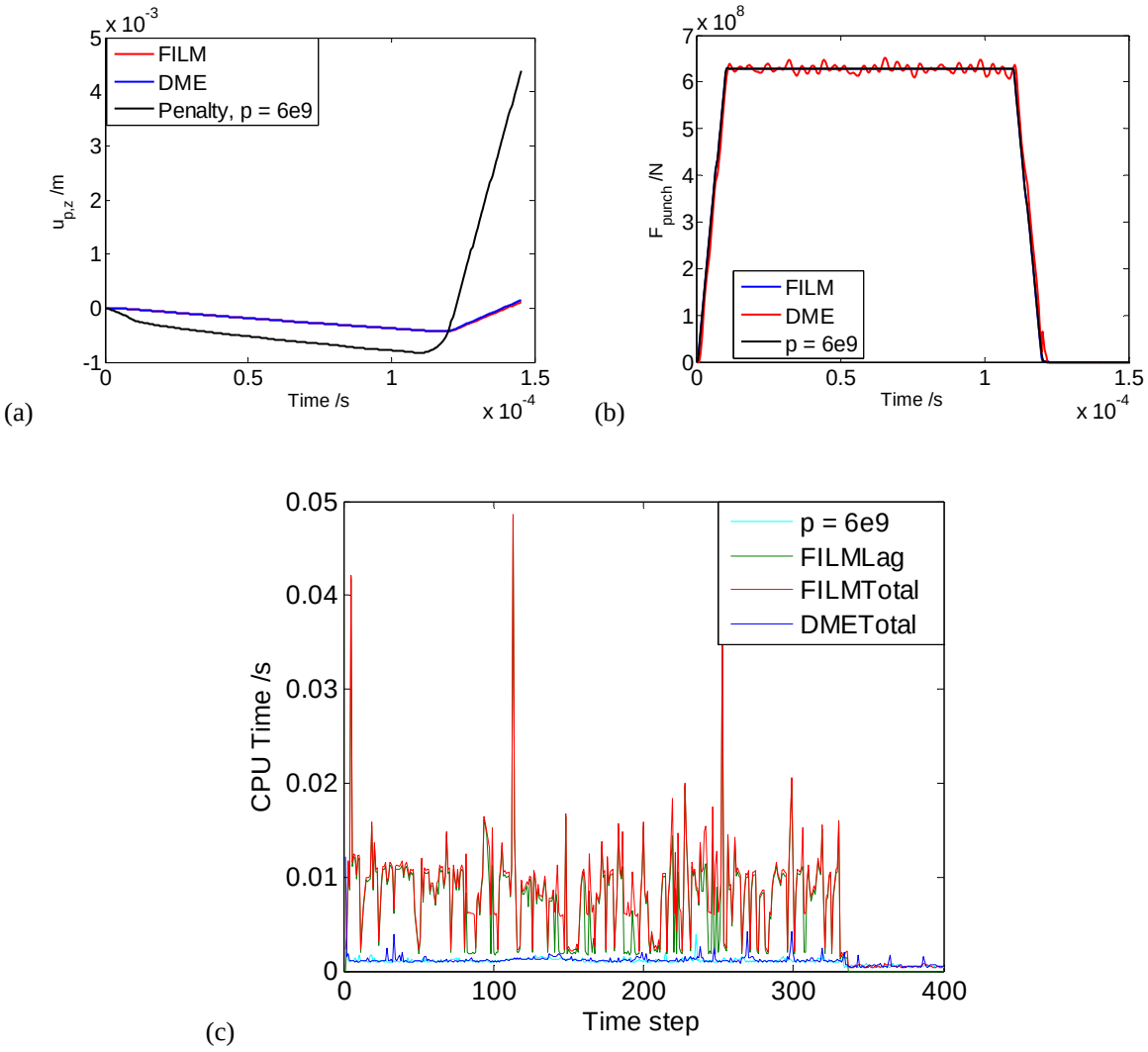

Figure 5: Punch penetration (a), contact force (b) and CPU times for contact solution (c) in Sim1.

According to Figure 5a the FILM and DME (Case 1) methods produce equal punch displacement during loading phase but slight, barely noticeable difference occurs during unloading. In contrast, the vertical displacement by Penalty method deviates considerably from the other methods. The value $p = 6\times10^9$, found by trial and error, gave the best results in this problem. The force resisting penetration, F_{punch}, is also quite similar to all methods besides the oscillations seen in the DME curve in Figure 5b. As for the CPU times (measured by Matlab tic function), it is seen that the time spend for contact computations by the DME and Penalty methods (DMETotal and p = 6e9) is about half of the lowest times by the FILM method. Moreover, most of the total time used by the FILM method is consumed in solving for the Lagrange multipliers from Equation (4), (compare the FILMLag and FILMTotal curves in Figure 5c). Finally, the FILM method displays heavy variations in CPU times which are attested by the high peaks in Figure 5c. Next, the results for Sim2 and Sim3 are shown in Figure 6.

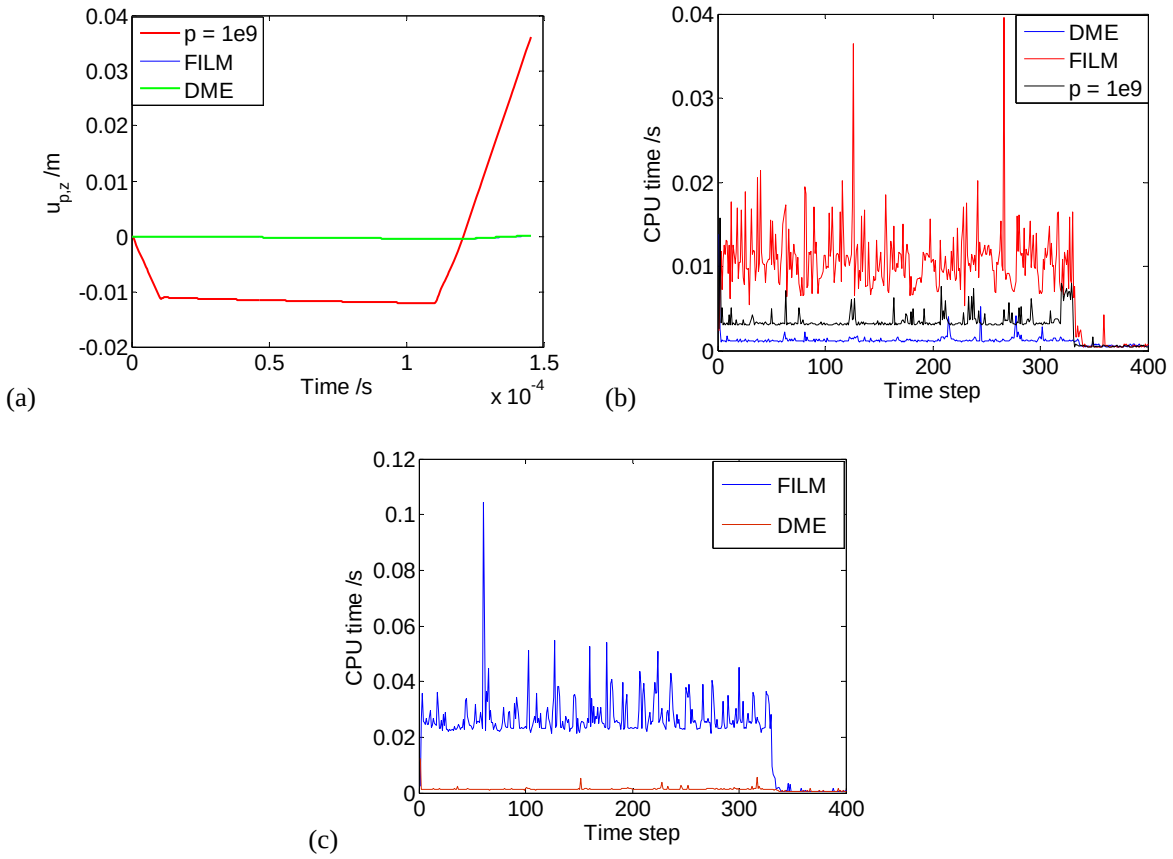

Figure 6: Punch penetration (a) and CPU times (b) in Sim2, and CPU times for contact solution (c) in Sim3

As the number of contact constraints increase, the Penalty method becomes more ill-behaving as seen in Figure 6a. In fact, no value of penalty coefficient giving reasonable results for punch displacement, $u_{p,z}$, was found in Sim3, i.e. when the number of contact constraints is 610. This deficiency of the penalty method is related to the relatively long contact interface in this problem: a value of the penalty coefficient giving good results close to the axis of symmetry is far too small, by many orders of magnitude, further away from it.

As to the CPU times spent in the contact computations, the DME method is clearly the most efficient one. Indeed, in Sim3, see Figure 6c, it is at least 20 times faster than the FILM method. It is also twice as fast as the Penalty method, as seen in Figure 6b.

In this specific problem, having 23036 DOFs, the second most time consuming operation during a time step is the computation of the internal force vector by $\mathbf{f}_{int} = \mathbf{Ku}$ where $\mathbf{K}$ is the global linear elastic stiffness (sparse) matrix. In the present simulations this time varied between 1 to 2 ms which is approximately of the same magnitude as the time needed to perform the contact computations with the DME method. Therefore, the efficiency of contact computations is crucial in this kind of explicit transient elasto-dynamics involving contact-impact.

3.2 Longitudinal impact of cylindrical bars

The problem of longitudinal impact of thick cylindrical bars described in Figure 7a is solved with the FILM, DME and Penalty methods in order to compare their performance. Axisymmetry of the problem is exploited and CST mesh shown for the left bar in Figure 7b is used. Relatively coarse mesh, with 406 for the left and 426 elements for the right bar is used.

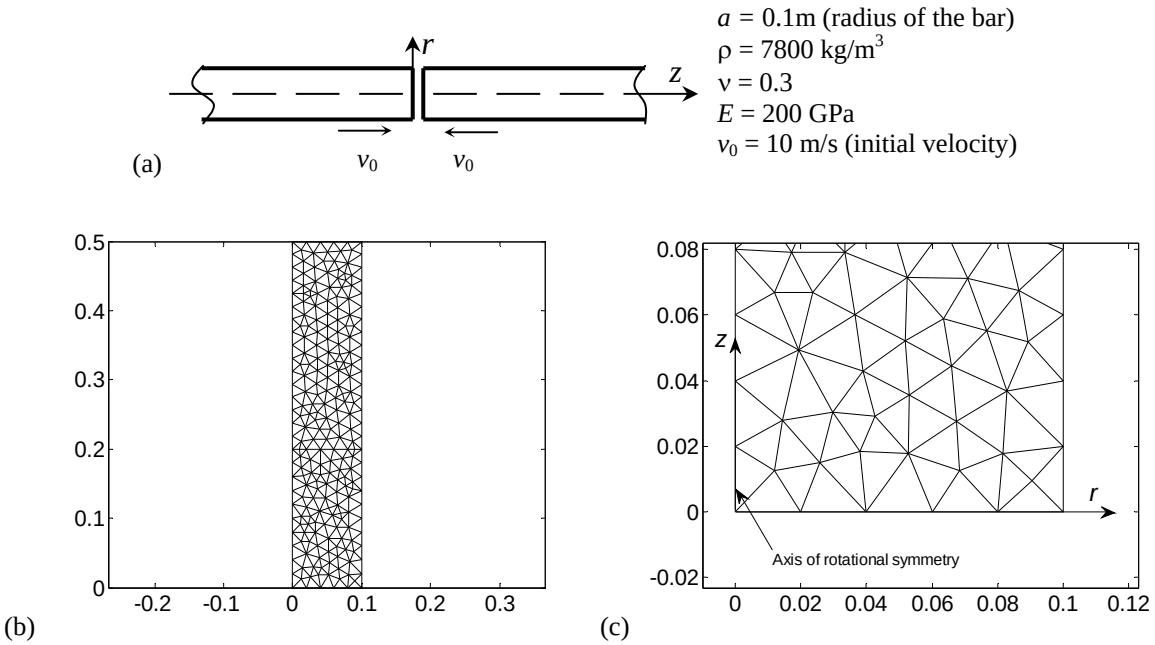

Figure 7: Longitudinal impact of thick bars (a), the CST mesh (b) and a detail (c).

The node-to-node contact interface is employed here and the contact computations are performed as explained in Section 2. The number of contact pairs is very small, 6 pairs, which is insignificant from the computational point of view. A time step $\Delta t = 1\times10^{-6}$ s is chosen to keep the computations stable. As the matrix $\Delta t^2\mathbf{G}\mathbf{M}^{-1}\mathbf{G}^{\mathrm{T}}$ is diagonal for the node-to-node contact interface, the average of its entries, 1.19×10^{10}, is taken for the penalty parameter. In the results in Figures 8-10, the gap computed as $\mathbf{G}\mathbf{u}^t - \mathbf{b}^t$ and contact forces are plotted at the contact nodes as a function of time for different methods.

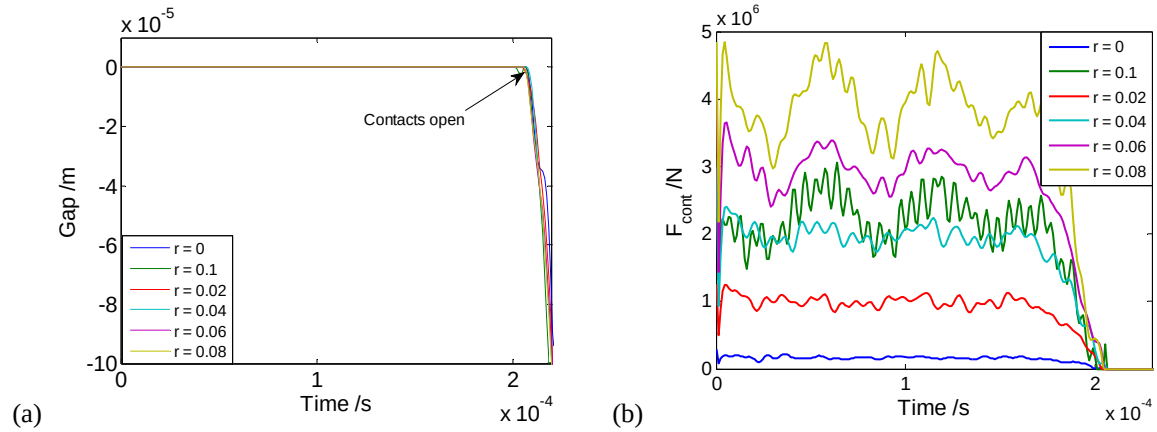

Figure 8: Simulation results with FILM method: gap (a), and contact forces (b).

According to the results in Figure 8, the impenetrability condition is accurately satisfied, i.e. the gap is zero all the time bars are in contact, with the FILM method. As the stress waves reflected at the free ends of the bars reach the contact surfaces, the contacts open and bars start to retreat. This event is indicated in Figure 8a. Next, the same results are presented for the Penalty method in Figure 9.

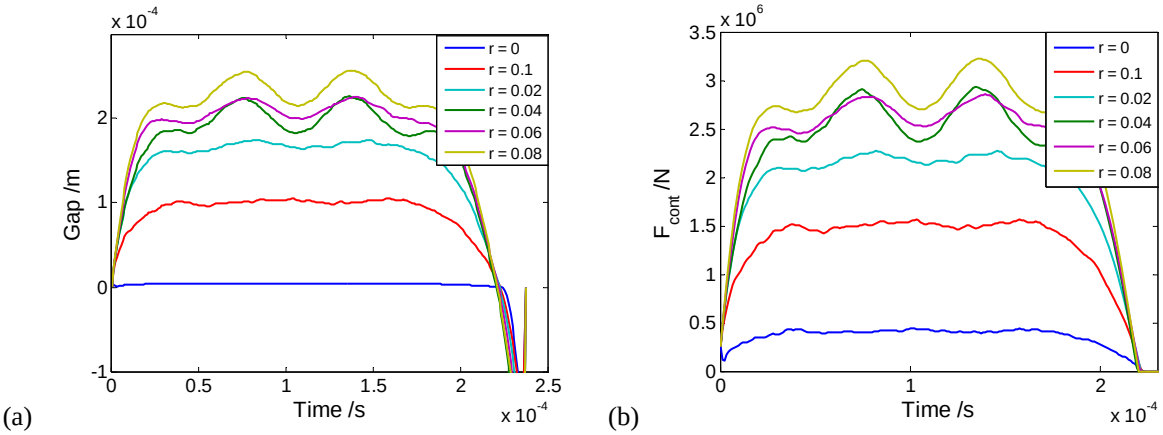

Figure 9: Simulation results with Penalty method ($p = 1.19\times10^{10}$): gap (a), and contact forces (b).

As expected, the Penalty method does not satisfy the impenetrability condition. Indeed, penetration occurs and the contact force is based on this penetration. Finally, the same results are presented for the DME method with the perfectly inelastic collision scheme ($e = 0$) in Figure 10.

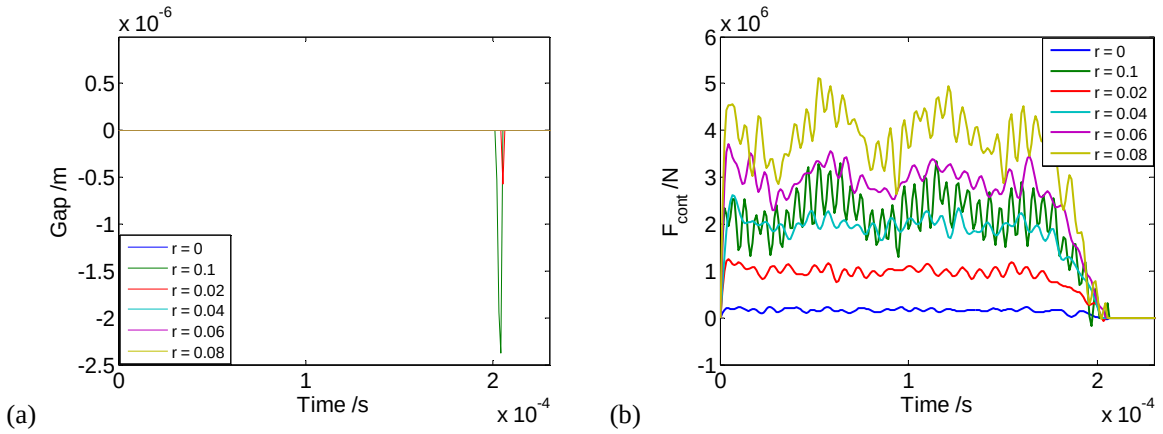

Figure 10: Simulation results with DME method: gap (a), and contact forces (b).

The results for the DME method with the perfectly inelastic collision assumption satisfy the impenetrability condition accurately, as attested by the zero gap values (see Figure 10a) until the arrival of the stress wave reflected from the free end of the bar. The contact forces in Figure 10b are somewhat similar to those produced with the FILM method.

Next, the methods are compared to the analytical solution of the problem by Valeš et al. [5]. The dimensionless axial stress at the location $r = 0.1$ m and $z = 0.2$ m, a location close enough to the contact surfaces so that the differences in the results between the methods are still visible (and not smoothed too much by the Saint-Venant principle). In addition, the different schemes for calculating the velocity of contact nodes with the DME method, Equation (10), are compared. The results are shown in Figure 11.

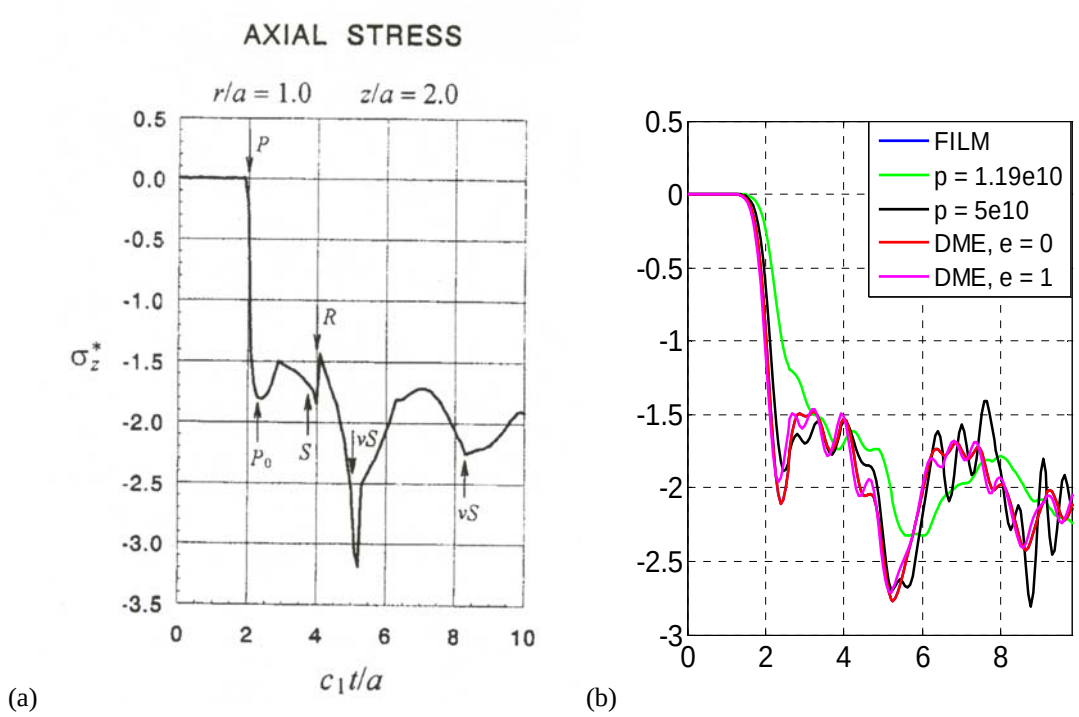

Figure 11: Analytical solution for dimensionless axial stress [5] (a), simulation results with different methods (b) and results with different velocity schemes of DME method (c).

As seen in Figure 11b, the axial stress predicted with the FILM and DME (e = 0) methods are identical. The result with the elastic collision scheme for velocity (DME, e = 1) deviates slightly from these. These methods predict the analytical solution with a good accuracy. For example, the arrivals of the different wave types are clearly identifiable in the numerical results as well. In contrast, the Penalty method with the value $p = 1.19\times10^{10}$ is quite poor when compared to the analytical solution. With the higher value, $p = 5\times10^{10}$, the Penalty method seems to perform slightly better first but then, after time station $c_1t/a = 5$, overshooting oscillations develop in the response. Moreover, this value provided poor results at the contact nodes.

4 CONCLUSIONS

- Different methods, including the forward increment Lagrange multiplier method (FILM), the Penalty method and the direct manifold elimination method (DME), to impose contact constraints in transient explicit dynamics were numerically compared in this paper.
- A method based on direct elimination of the contact constraints was developed and tested for the node-to-node contact interface. The theoretical background of the method based on the theory of manifolds was elaborated with some detail.
- In the numerical simulation of the indentation problem with a rigid punch, the DME method was found to be overwhelmingly more efficient than the FILM method while both methods provided similar results. As to the Penalty method, while efficient, it failed to produce reasonable results when the contact interface was relatively wide. It is more suitable for point-like contact problems. Moreover, the Penalty method has an adverse effect on the numerical stability of the explicit integration and the problem specific pain to find the correct value of the parameter.

- In the impact problem of longitudinal bars, the FILM and DME methods predicted the analytical solution for axial stress with a good accuracy. These methods, the DME with the perfectly inelastic collision assumption, satisfied the impenetrability condition accurately and predicted identical results for axial stress. In contrast, the results with the Penalty method deviated from the analytical solution and from the other methods as well.
- Due to its efficiency and accuracy, the DME method can be regarded as superior to the FILM method in problems where the FILM method requires a solution of coupled system of equations for the Lagrange multiplier. These problems include the rigid punch indentation simulated in this paper and problems with a more general contact interface.
- In the future developments of the DME method, it will be formulated for more general node-to-segment contact interfaces.

REFERENCES

[1] N.J. Carpenter, R.L. Taylor M.G. Katona, Lagrange Constraints for Transient Finite Element Surface Contact. *International Journal for Numerical Methods in Engineering*, **32**, 103-128, 1991.

[2] J.M. Mäkinen, Manifolds on Continuum Mechanics. In: A. Koppel & J. Oja Eds. *Continuum Mechanics*, Nova Science Publishers. pp. 1-52, 2010.

[3] T.J. Saksala, J.M. Mäkinen, Numerical Modelling of Bit-Rock Interaction in Percussive Drilling by Manifold Approach, In: A. Eriksson and G. Tibert Eds. *Proceedings of the 23rd Nordic Seminar on Computational Mechanics*, KTH Stockholm, Sweden, October 21-22, 2010.

[4] G. D. Hahn, A Modified Euler Method for dynamical analyses. *International Journal for Numerical Methods in Engineering*, **32**, 943 – 955, 1991.

[5] F, Valeš et al., Wave Propagation in a Thick Cylindrical Bar Due to Longitudinal Impact. *JSME International Journal, Series A: Mechanics and Material Eng*, **39**, 60 – 70, 1996.